Paper 77

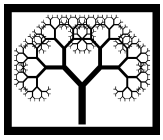

Proceedings of the Eleventh International Conference
on Computational Structures Technology,
B.H.V. Topping, (Editor),
Civil-Comp Press, Stirlingshire, Scotland

A Method to Detect and Assess Damage in Beams based on Frequency Changes

G.-R. Gillich, Z.-I. Praisach and D. Amariei
Department of Mechanical Engineering
University "Eftimie Murgu" of Resita, Romania

Abstract

This paper presents a new method for damage detection in beam-like structures and assessment of their location and severity based on a shift in natural frequencies, by considering the particular manner in which the natural frequencies of the first ten bending vibration modes change as a result of the occurrence of damage. Prior research revealed the influence of cross-section reduction on changes of strain energy and consequently natural frequencies of various bending vibration modes; this influence is formalized, a mathematical relation being worked out. The proposed method became a pattern recognition problem, the measured frequency changes being compared with values analytically determined. Numerous experiments made on real beams confirmed the validity of the method.

Keywords: damage detection, beam, crack, vibration, natural frequency, shape mode, strain energy.

1 Introduction

Regular inspection and control of engineering structures is necessary in order to detect damages in real time and determine the safety and reliability of the structure. Early damage identification allows properly programmed maintenance with impact on exploitation costs diminution, or the putting out of operation and replacement to avoid accidents. A large series of non-destructive methods based on the influence of damage upon the dynamic behaviour of structures were developed [1]. These so-called dynamic methods, due to their global perspective, are able to indicate the appearance of possible damages even in large structures, by identifying changes of their mechanical or dynamic characteristics such as natural frequencies [2, 3 and 4], mode shapes, mode shape curvature/bending strain [5, 6 and 7], damping ratio, and stiffness or flexibility [8 and 9]. The features on which damage detection stands are obtained mainly from acceleration or strains measurements.

Existing dynamic methods were developed for specific applications proving their utility with certain limitations in real environment. Reviews of vibration-based damage identification methods [10] reveal some critical issues weaknesses about their usage and highlight the research directions to be followed. Taking in consideration these remarks, our research was oriented to the use of continuous models, which allows a better phenomena understanding [11], leading to increased precision in assessing damages along with the possibility of involving a singular sensor.

2 Influence of damage upon beam dynamic behaviour

2.1 Numerical investigation

Investigations using the finite element method were performed on a beam in four support type cases: cantilever, double clamped, simply supported and fixed-pinned. The steel beam (rectangular prism) had the following geometrical characteristics: length L = 1000 mm; width B = 50 mm and height H = 5 mm. Consequently, in the initial estate, we had the beam cross-section $A = 250 \cdot 10^{-6}$ m^2 and the moment of inertia $I = 520.833 \cdot 10^{-12}$ m^4. As material parameters we have considered the mass density ρ = 7850 kg/m^3; modulus of elasticity $E = 2.0 \cdot 10^{11}$ N/m^2 and Poisson's ratio μ = 0.3. Additionally, the damage estate introduced three new parameters: damage location $c = x/L$, depth δ and width W = 2 mm.

In order to gain a clear picture about the entire phenomena which occur by the appearance of an open crack, simulations for the undamaged and a series of damaged beams were performed [11]. The 3D beam was meshed by 2 mm elements in all cases; in the vicinity of damages, which were placed one by one along the beam length (around 200 locations) and with different levels of depth (reducing the cross-section from 8 to 75 %), the mesh was defined with finer elements. For all the cases were determined the first ten natural frequencies of the weak-axes bending vibration modes, used to highlight the frequency changes in a graphical way (see Figures 1 and 2). For each diagram the axes of the horizontal plane have assigned the beam length and damage depth, while the vertical axe has assigned the corresponding frequency.

The analysis of the natural frequency distribution related to damage location and depth permitted the formulation of some remarks, used as start point for the development of the method, listed below:

1. For each vibration mode and support type, there are certain points on the beam where damage does not produce any changes in natural frequency, irrespective to damage depth; their number for different support types and vibration modes is given in table 1.

2. For each vibration mode and support type, there are certain points on the beam in which natural frequency changes due damage exhibit local extreme; their number for different support types and vibration modes is also shown in table 1. In this case, damage depth amplifies the frequency changes.

Points in which:	Cantilever beam	Double clamped	Simply supported	Fixed-pinned
no change of natural frequency occur	i	i	i+1	i+1
the change of frequency exhibit minima	i	i+1	i	i+1

Table 1. Number of typical points on the beam for the frequency changes curves

This leads to the conclusion that stiffness reduction in a transversal slice of the beam does not conduct automatically to frequency changes (ex. mid-span of simply supported beam in pair vibration modes – see Figure 2.a). In other words, the same damage placed in two different locations produce different effects upon the natural frequency of the beam for a certain vibration mode.

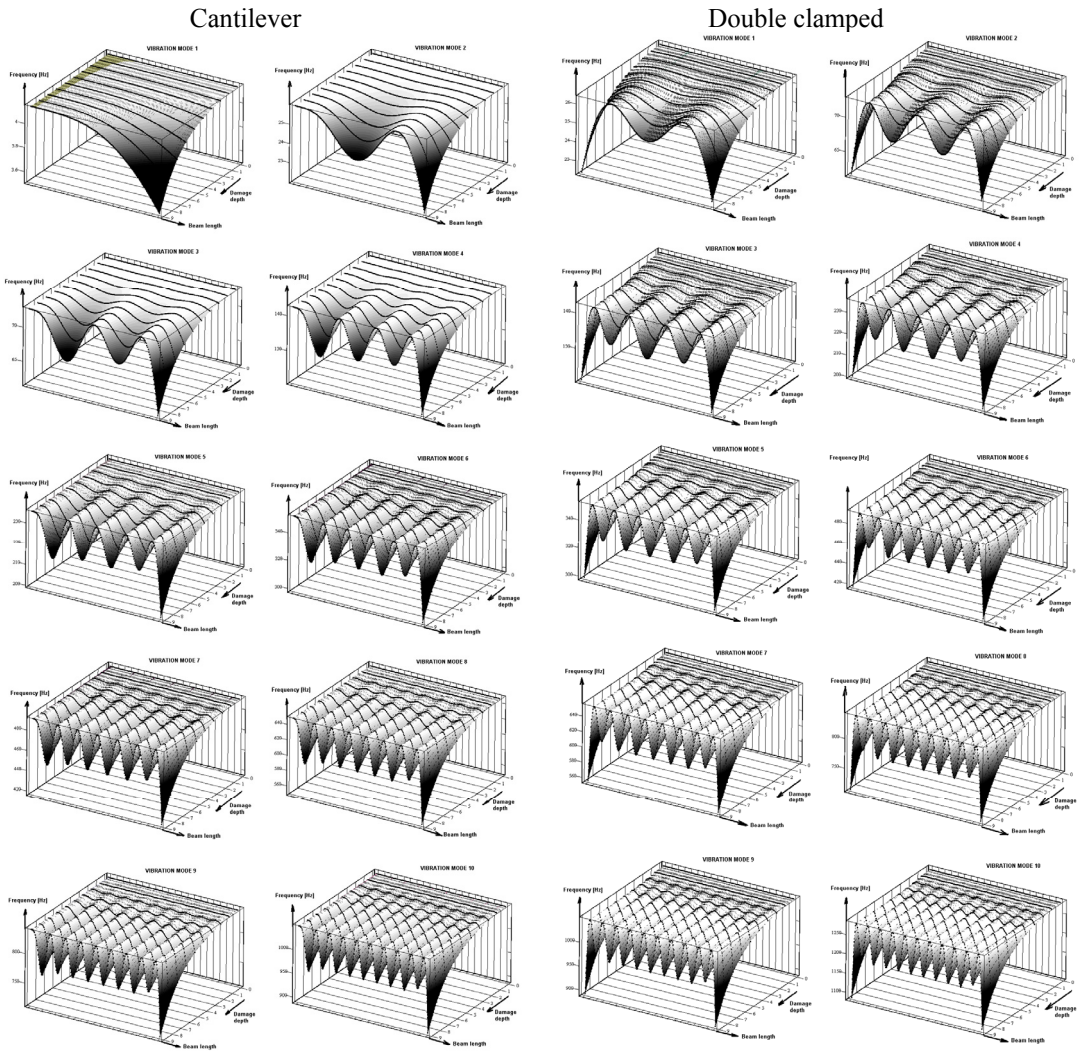

a. b.

Figure 1: Frequency changes for the first ten weak-axes bending modes for the cantilever (a.) and double clamped (b.) beam.

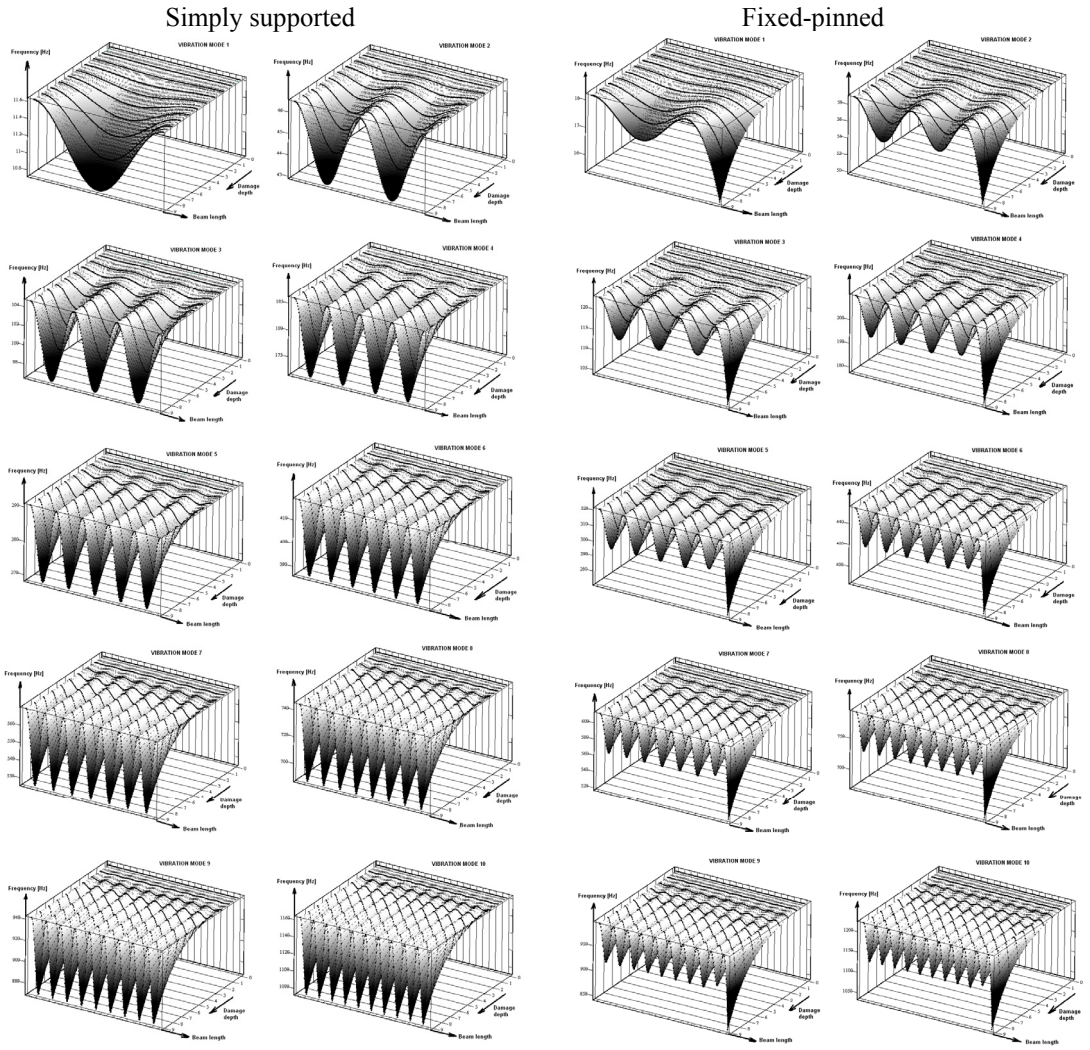

Figure 2: Frequency changes for the first ten weak-axes bending modes for the simply supported (a.) and fixed-pinned (b.) beam.

On the other hand, damage placed on the same location produce different effects in different vibration modes (ex. in mid-span of simply supported beam in 1st and 2nd vibration mode – see Figure 2.a).

Comparing these typical points with the ones of corresponding mode shape $\phi_i(x)$ and mode shape curvature $\phi_i''(x)$ of the undamaged beam, similitude is obvious (ex. 4th mode in Figure 1.a and 3).

This revealed that in the points where the mode shape is null, no frequency changes occur because in that locations the slices present only rotation, without any bending and displacement, while in the points of local extreme bending and displacement exhibit maxima, producing the highest frequency changes around that location (see Figure 3).

Simulations depictured for all analyzed cases that the algorithm is available, even for various temperature conditions or beam imprinted acting strains.

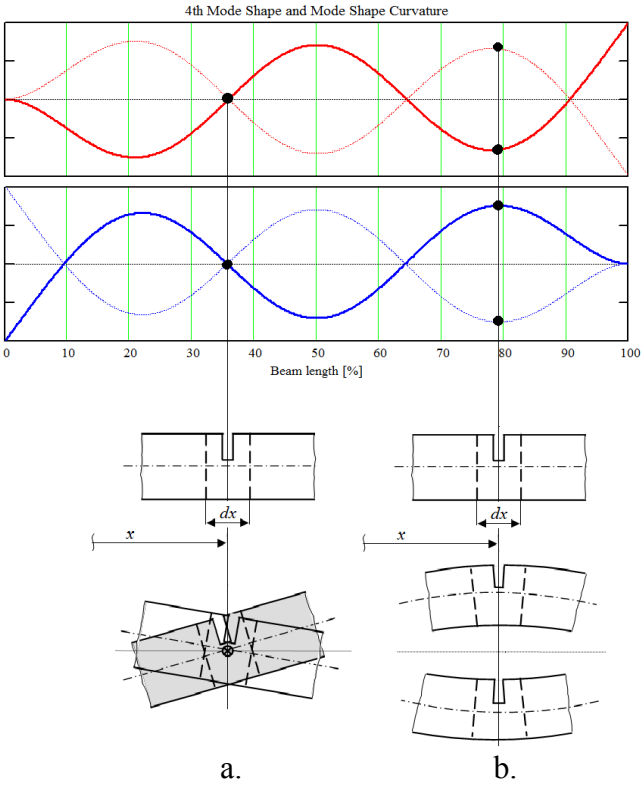

Figure 3: The effect of bending on slices placed on inflection points and local extreme respectively – ex. for the 4th vibration mod of a cantilever.

These presumptions are also supported by the strain energy relation of a slice:

$$dU_i(x) = \frac{1}{2} EI\left(\phi_i''(x)\right)^2 dx \tag{1}$$

which proves that slices placed in inflection points of the mode shape curvature do not store energy. Therefore, a cross-section reduction produces no changes in the beam dynamic behaviour, so that no natural frequency shift occurs.

On the other hand, Equation (1) confirm that the stored energy in a slice placed on a extreme point of the mode shape reach the highest value in its vicinity, while the mode shape curvature gets highest values on that point. Between inflection points and extreme points, the stored energy and consequently the frequency changes take values between zero and maxima, depending on the square value of the mode shape curvature $\phi_i''(x)$.

Beside this remarks, one observe that the frequency changes produced on any locations on the beam are proportional to the cross-section reduction, as presented in Figure 4 in all four analyzed cases.

All presented above stands at deeply understanding of entire phenomena and constituted the basis for elaboration of a mathematical model, as well as ground of our methodology.

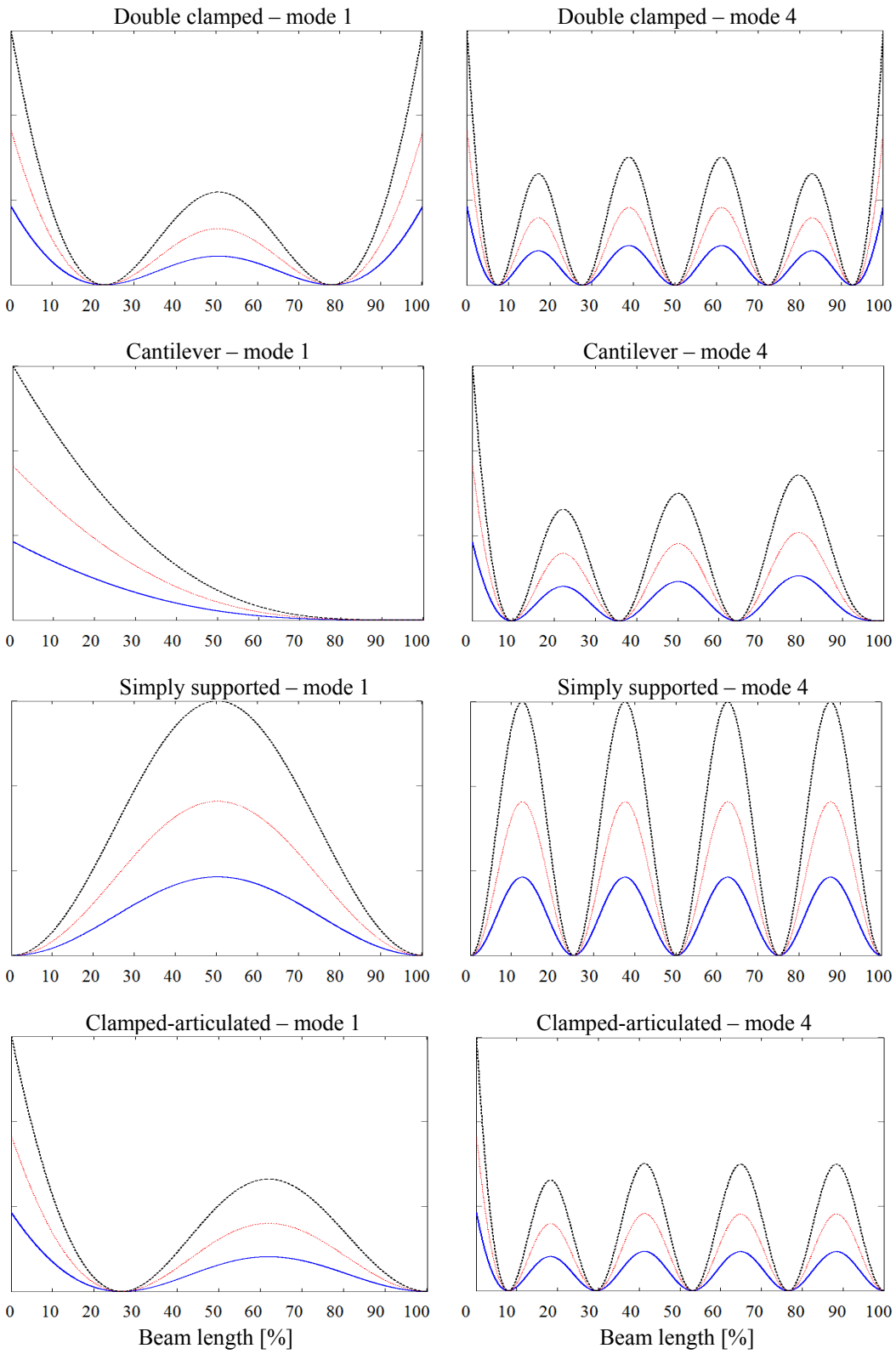

Figure 4: Frequency changes for different depth levels.

2.2 Mathematical model

Based on the phenomena highlighted above, following numerous attempts, we reached the relation bellow, defining the frequency shift for the weak-axes bending vibration mode *i* due to damage, as follows:

$$\left|\Delta f_i(x)\right| = f_{i\_U} - f_{i\_D}(x) = f_{i\_U} \cdot k_\alpha \cdot \frac{k_s \cdot H}{L} \cdot \left(\frac{\delta}{H-\delta}\right)^{\frac{3}{2}} \cdot \frac{k_b \cdot \overline{G} \cdot \overline{L}^2}{6} \cdot \left(\overline{\phi_i''}(x)\right)^2 \qquad (2)$$

The right expression of Equation (2) contains information extracted from the undamaged beam, excepting the damage location x and depth δ. It has to be mentioned that this equation is valid for all vibration modes and support types as it is, without other alterations being necessary.

Equation (2) reveals the influence of each factor on frequency changes. ***Temperature*** influence is considered by k_α coefficient; for ambient temperature 22° this takes the unit value.

The influence of beam ***geometrical dimensions*** is provided by the height *H,* weighted by shape coefficient k_s, and length *L*.

The influence of the ***cross-section reduction*** is represented by the bracket term; as expected, the enlargement of damage depth δ amplifies the frequency shift.

The ***boundary conditions*** (beam support type) are represented in the relation by the sum of areas of bending moments acting on the beam, calculated for normalized weight $\overline{G}$ and length $\overline{L}$, weighted with k_b coefficient placed in the third fraction. For the cantilever beam k_b = 1 as well as for the simple supported and the double clamped one. For the beam clamped at one end and pinned at the other it is 0.875.

Damage ***location*** influence is introduced by the square of the normalized mode shape curvature; $\left(\overline{\phi_i''}(x)\right)^2 = 0\ldots1$. Obvious, at the location x for which $\left(\overline{\phi_i''}(x)\right)^2 = 1$, highest frequency shift is achieved for the corresponding vibration mode. In this case, a coefficient *k* can be defined as:

$$k = k_\alpha \cdot \frac{k_s \cdot H}{L} \cdot \left(\frac{\delta}{H-\delta}\right)^{\frac{3}{2}} \cdot \frac{k_b \cdot \overline{G} \cdot \overline{L}^2}{6} \qquad (3)$$

is constant for a given beam with certain damage, irrespective to vibration mode number *i*. The mode shape curvature is the only factor controlling the influence of damage location; meanwhile the *k* coefficient from Equation (3) indicates the influence of damage depth.

Figures 1 and 2 along with Equation (2) point that certain crack placed in a particular beam location provide a unique series of frequency shifts for specific beam support type. As exception we nominate the case of symmetric supported beams, where two cracks placed symmetrically to the beam mid-span produce the same effect.

Since Equation (2) established a biunivocal relation between natural frequency shift and mode shape curvature of the undamaged beam, similar series can be obtained from the mode shape curvature, constituting patterns defining the location.

3 Damage detection and assessment algorithm

3.1 Method description

The proposed method covers the first tree levels of damage identification defined by Rytter [13], following steps being necessary to be covered in order to achieve this.

1. The first ten natural frequencies of the weak-axes bending vibration modes for the undamaged beam have to be determined. The series

$$A:\{ f_{1\_U};\ f_{2\_U}; f_{3\_U}; f_{4\_U}; f_{5\_U}; f_{6\_U}; f_{7\_U}; f_{8\_U}; f_{9\_U}; f_{10\_U} \}$$

results. In case of older structures, the actual status of the beam can be considered as start point, neglecting the possible existing cracks. Thus, only the evolution of new or developing cracks can be assessed.

2. For the same vibration modes the frequencies have to be measured periodically. For each choose moment a series

$$S:\{ f_{1\_D};\ f_{2\_D}; f_{3\_D}; f_{4\_D}; f_{5\_D}; f_{6\_D}; f_{7\_D}; f_{8\_D}; f_{9\_D}; f_{10\_D} \}$$

is obtained.

3. Comparison with the initial estate has to be performed. The series

$$D:\{ \Delta f_1;\ \Delta f_2; \Delta f_3; \Delta f_4; \Delta f_5; \Delta f_6; \Delta f_7; \Delta f_8; \Delta f_9; \Delta f_{10} \}$$

ensue. Differences representing frequency shift Δf_i indicate ***damage appearance.***

4. The relative frequency shift is determined by dividing the values of D series to the one of A. Results the series R

$$R:\{ \Delta f_1^*;\ \Delta f_2^*; \Delta f_3^*; \Delta f_4^*; \Delta f_5^*; \Delta f_6^*; \Delta f_7^*; \Delta f_8^*; \Delta f_9^*; \Delta f_{10}^* \}$$

5. The values of the R series have to be normalized, by dividing all values of the series by the highest one. It results

$$N:\{ \Delta \bar{f}_1;\ \Delta \bar{f}_2; \Delta \bar{f}_3; \Delta \bar{f}_4; \Delta \bar{f}_5; \Delta \bar{f}_6; \Delta \bar{f}_7; \Delta \bar{f}_8; \Delta \bar{f}_9; \Delta \bar{f}_{10} \}$$

The series' elements take positive subunit values. Normally, only one element takes the unit value.

6. Series representing square of the mode shape curvature $\left(\overline{\phi_i''(x)}\right)^2$ for various locations on the beam are determined, resulting

$$C:\{ \left(\overline{\phi_1''(x)}\right)^2; \left(\overline{\phi_2''(x)}\right)^2; \left(\overline{\phi_3''(x)}\right)^2; \left(\overline{\phi_4''(x)}\right)^2; \left(\overline{\phi_5''(x)}\right)^2; \left(\overline{\phi_6''(x)}\right)^2;\ \ldots; \left(\overline{\phi_{10}''(x)}\right)^2 \}$$

7. Resulted N series is compared with the determined C series. The x coordinate of the mode shape curvature which provides the best fit to frequency change series, indicates the ***damage location***.

8. Ratio between values of N and C series has to be determined to obtain the value of coefficient k presented in Equation (3).

9. ***Damage depth*** δ can be now extracted as single unknown in this relation.

10. Two values δ_{inf} and δ_{sup} around damage depth are picked. For those values, considering the x coordinate, the relative frequency shift chart is plotted, together with the one of the measurements.

11. It is searched if the measured frequency shifts are well framed by the analytically determined ones.

12. In case of satisfactory results, a fine tuning can be made, by relocating coordinate x around already found location. If unsatisfactory results, a new coordinate x is searched again and steps 7 to 11 has to be reload.

To exemplify the method we chose the case of a double clamped beam, having damage placed at $c = 0.6x/L$ from the left end. The measurement results (series A) obtained for the undamaged beam are presented in Table 2.

Mode number	1	2	3	4	5
Measured frequency [Hz]	26.099	71.926	140.991	233.070	348.205
Mode number	6	7	8	9	10
Measured frequency [Hz]	486.420	647.735	832.155	1039.672	1270.254

Table 2. Measured natural frequencies for undamaged beam

Table 3 show the measurement results (series S) in case of a crack occurrence at $c = x/L$. The series D, representing the frequency shift as differences $f_{i\_U} - f_{i\_D} = \Delta f_i$, results. The ratio between series D and series A provide the relative frequency shift (series R).

Mode number	1	2	3	4	5
Measured frequency [Hz]	25.929	71.493	140.579	230.016	348.130
Mode number	6	7	8	9	10
Measured frequency [Hz]	481.188	643.729	829.675	1026.964	1269.934

Table 3. Measured natural frequencies for a beam damaged at $c = 0.6$

Series R values divided by own highest value offers, according to step 5, the normalised relative frequency shifts (series N), given in Table 4 and depictured in Figure 6.b.

Mode number	1	2	3	4	5
Measured frequency [Hz]	0.497	0.459	0.223	1.000	0.016
Mode number	6	7	8	9	10
Measured frequency [Hz]	0.821	0.472	0.228	0.933	0.019

Table 4. Normalised relative frequency shifts for measurement data (crack at $c = 0.6$)

Resulted measurements are presented under graphical form in Figure 5. We can highlight appearance of different frequency shifts, not in a scaled manner, for different vibration modes [14].

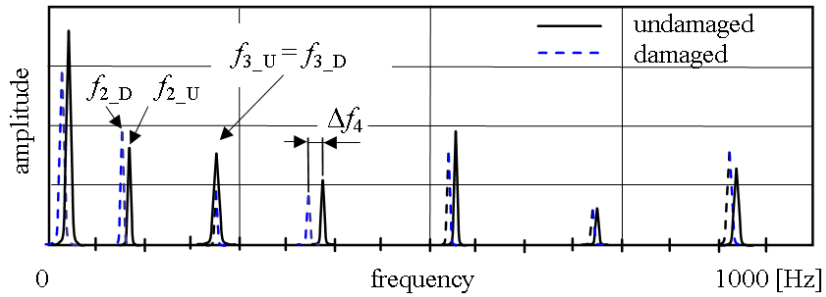

Figure 5: Frequency spectrum of undamaged and damaged beam.

Follow to all these 5 steps covered, the square of the mode shape curvature has to be determined; characteristic curves are showed in Figure 6. A cross plan, on which the projection of the square mode shape curvature for all ten modes are revealed, scan the entire length of the beam. Figure 6 shows also the example of the plan situated at $x/L = 0.6$ containing the afferent projection.

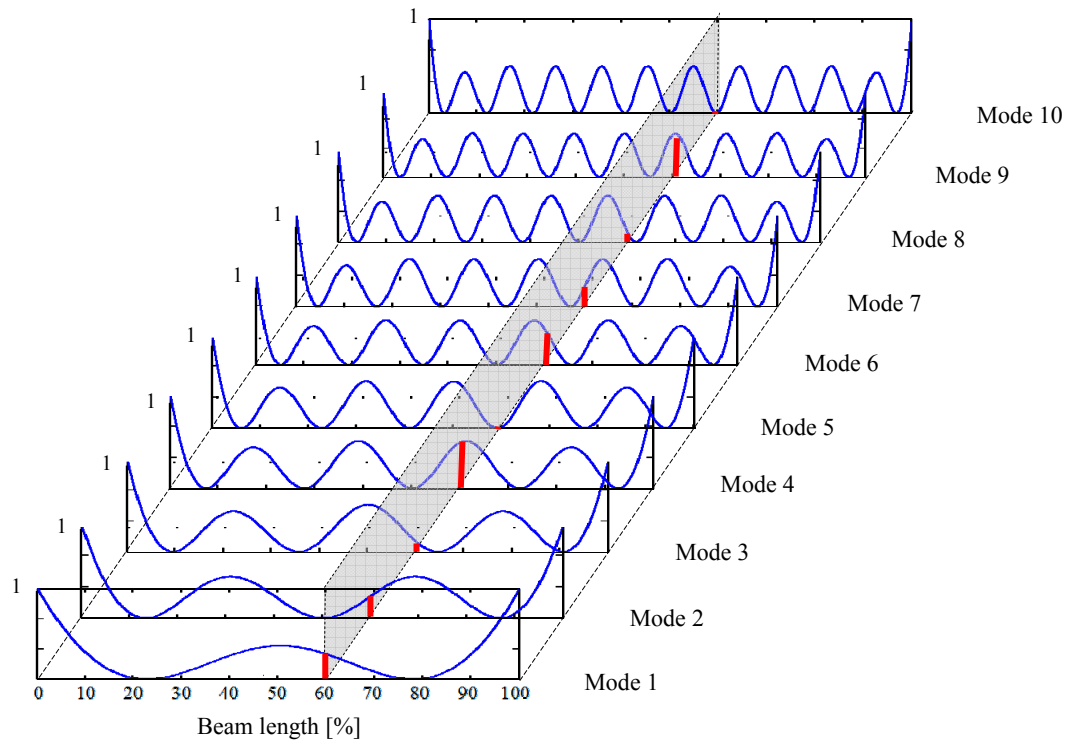

Figure 6: Square of the mode shape curvatures of the first ten vibration modes for the double clamped beam and the cross plan containing their values for $x/L = 0.6$

Resemblance between square mode shape curvature values (Figure 7.a) and the normalized relative frequency shifts (Figure 7.b) can be easily observed, leading to the conclusion that damage is placed at 600 mm form the beam's left end. For automatic detection, pattern recognition algorithms can be involved.

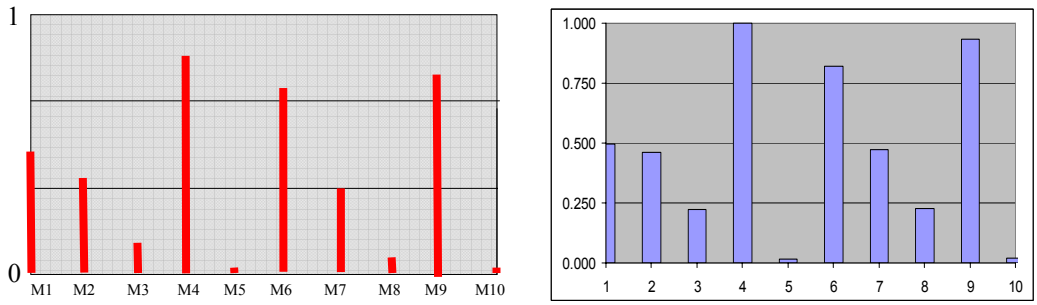

a. b.

Figure 7: Square of the mode shape curvatures $x/L = 0.6$ and the normalized relative frequency shift chart (b.) of a double clamped beam with damage at $x/L = 0.6$

Due to beam symmetry, the same configuration of normalized relative frequency shift can appear on the plan for $x/L = 0.4$, as presented at the end of Subsection 2.2.

3.2 Experiments and method validation

To validate the method availability, we developed a series of experiments. As specimens, 12 steel beams similar with the one presented in figure 7 were used, having the geometrical and mechanical characteristics described in Subsection 2.1. During the tests, the beams where fixed in a milling machine vise, which assured optimal fixing conditions. The structure excitation for determining the natural frequency was realised both by hammer hitting and pushing out of the equilibrium position; for the same beam, the results were similar. The measurement system composed by a laptop, a NI cDAQ-9172 compact chassis with NI 9234 four-channel dynamic signal acquisition modules and a Kistler 8772 accelerometer mounted on the free end of the beam was used (Figure 8).

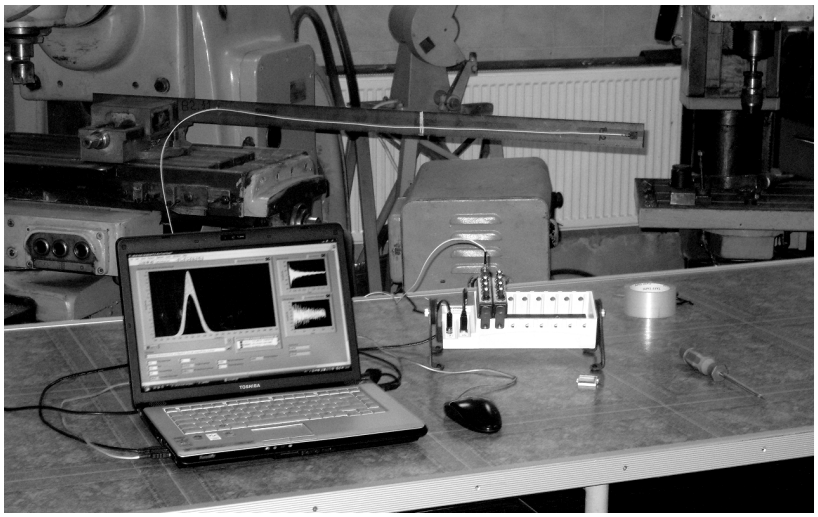

Figure 8: Normalized frequency shift chart representing the first ten bending

Experiments were conducted for determination of the undamaged beam first ten natural frequencies, and, afterwards, the changes owed to different types of damages appearance. The damages were made by saw cutting, the cuts being approximately 2 mm wide. For defect simulation, initially was made a cut with the depth of around 33%, then the depth was increased to approximately 66%. We performed five sets of measurements for each beam, both for the undamaged case and for the two cases with damages. Constantly the results allowed the location of the damage with a precision higher than 1%, namely an error less than 10 mm.

Table 5 presents the normalized relative natural frequency shifts for both damage depth levels (N1 and N2) and the square of mode shape curvatures (C) for location $x/L = 0.569$, which best fits these data series. Measurement errors can be observed, because the two series Figure 9 shows the results obtained based on this table values.

Mode number	Determined by measurements for cca. 33% depth	Determined by measurements for cca. 66% depth	Determined with $\left(\overline{\phi_i''(x)}\right)^2$
i	N1	N2	C
1	0.116	0.149	0.096
2	1	1	0.825
3	0.264	0.272	0.239
4	0.502	0.499	0.418
5	0.615	0.625	0.531
6	0.114	0.095	0.111
7	0.865	0.904	0.753
8	-0.009	-0.052	0.001
9	0.752	0.853	0.718
10	0.169	0.182	0.163

Table 5. Square of shape mode curvatures of the undamaged beam and the normalized relative natural frequency shifts for a beam having a damage located at $x = 569$ mm from the clamped end.

To detect the first depth level produced by the simulated crack, the values of the relative frequency shift series (R) are divided by the values of the normalized frequency shift series (N1). Result ten values of the *k* coefficient, having the average 1.3531768 after elimination of abnormal values.

For the second depth level, following the same algorithm, the found coefficient is $k = 4.0283731$.

From Equation (3) we computed depth δ = 1.86 mm and δ = 2.75 mm respectively.

Figures 10 and 11 prove the correct damage location and assessment for both estates, square of mode shape curvature for 33% and 42%, respectively 50% and 58% (dashed lines) framing the measured values (continuous lines). Dimensional measurement confirmed these results.

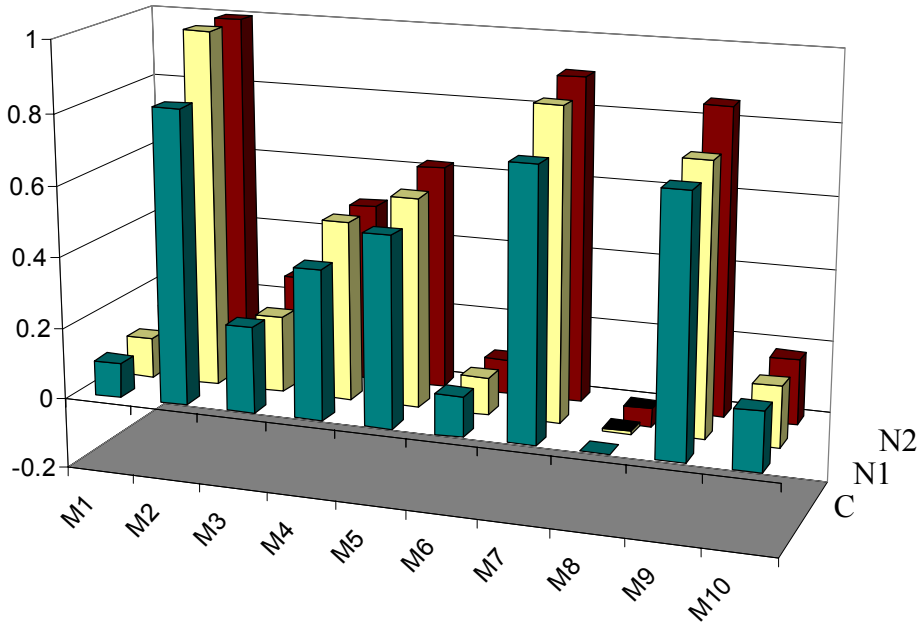

Figure 9: Square of shape mode curvatures of the undamaged beam and the normalized relative natural frequency shifts for a beam having a damage located at x = 569 mm from the clamped end

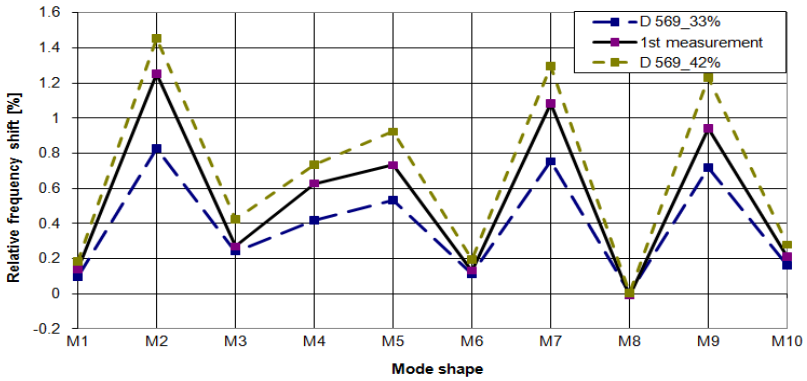

Figure 10: Damage location and depth evaluation for first depth level

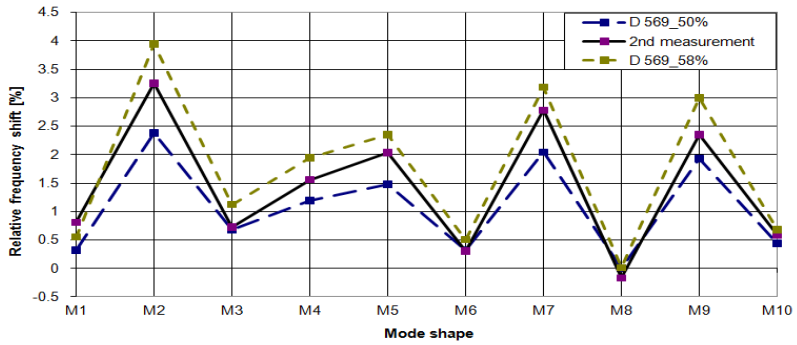

Figure 11: Damage location and depth evaluation for second depth level

4 Conclusion

Studying the literature it is noticed that, in spite of the multiple manners of approaching of the damage detection issue, no precise methods, applicable in real conditions and implying few numbers of measurement points have been developed.

The proposed method, applicable to beams with open cracks, is based on certain phenomena characteristic to beams dynamic behaviour, resulted from several analytical, numerical and experimental studies by the authors.

The conclusions of the studies are:

- changes in natural frequencies of beams, due to damage, are significantly influenced by damage location, while depth just amplifies this effect;
- for cracks situated on inflexion points of the mode shape, corresponding natural frequency remains unchanged, irrespective of the damage depth;
- along the beam, the stored energy and consequently the frequency depend on the square value of the mode shape curvature;

For damaged beams the method provides unique solution; for symmetrically supported beams, the method offers two symmetrical solutions, only one being the real one.

Crack location was determined with approximately 1% precision without requiring laboratory special conditions, standing on the use of one single accelerometer, appropriate for practical applications.

Acknowledgements

The authors gratefully acknowledge the support of the Managing Authority for Sectoral Operational Programme for Human Resources Development (MASOPHRD), within the Romanian Ministry of Labour, Family and Equal Opportunities by co-financing the project “Excellence in research through postdoctoral programmes in priority domains of the knowledge-based society (EXCEL)” ID 62557.

References

[1] D. Balageas, C.P. Fritzen, A. Güemes, “Structural health monitoring”, ISTE Ltd, London, 2006.

[2] P. Cawley, R.D. Adams, “The location of defects in structures from measurements of natural frequencies”, Journal of Strain Analysis, 14(2), 49-57, 1979.

[3] S.W. Doebling, C.R. Farrar, M.B. Prime, D.W. Shevitz, “Damage identification and health monitoring of structural and mechanical systems from changes in their vibration characteristics: a literature review”, Reprot No. LA 13070-MS, Los Alamos National Laboratory, Los Alamos, NM, 1996

[4] O.S. Salawu, “Detection of structural damage through changes in frequency: a review”, Engineering Structures, 19(9), 718-723, 1997.
[5] W.M. West, “Illustration of the use of Model Assurance Criterion to detect structural changes in an orbit test specimen”, Proceedings of Air Force Conference on Aircraft Structural Integrity, 1-6, 1984.
[6] A. K. Pandey, M. Biswas, M.M. Samman, “Damage detection from changes in curvature mode shapes”, Journal of Sound and Vibration 145, 321–332, 1991.
[7] N. Stubbs, J.-T. Kim, K. Topole, “An Efficient And Robust Algorithm For Damage Localization In Offshore Platforms,” in Proc. ASCE Tenth Structures Congress, 543–546, 1992.
[8] U. Lee, J. Shin, “A frequency response function-based structural damage identification method”, Computers and Structures 80, 117–132, 2002.
[9] A.K. Pandey, M. Biswas, “Damage Detection in Structures Using Changes in Flexibility”, Journal of Sound and Vibration, 169, 3-17, 1994.
[10] Scott W. Doebling, Charles R. Farrar, and Michael B. Prime A SUMMARY REVIEW OF VIBRATION-BASED DAMAGE IDENTIFICATION METHODS, Engineering Analysis Group, Los Alamos National Laboratory Los Alamos, NM
[11] Z.-I. Praisach, G.-R. Gillich, D.E. Birdeanu, “Considerations on Natural Frequency Changes in Damaged Cantilever Beams Using FEM”, Latest Trends on Engineering Mechanics, Structures, Engineering Geology, 214-219, 2010.
[12] G.-R. Gillich, Z.-I. Praisach, “Robust method to identify damages in beams based on frequency shift analysis”, SPIE Smart Structures/NDE, 8348-47, San Diego, California, USA, 2012.
[13] A. Rytter, “Vibration based inspection of civil engineering structures”. Ph.D. Thesis, Aalborg University, Denmark, 1993
[14] G.-R. Gillich, Z.-I. Praisach, C.M. Iavornic, “Reliable method to detect and assess damages in beams based on frequency changes”, Proceedings of the International Design Engineering Technical Conferences & Computers and Information in Engineering Conference IDETC/CIE 2012, Chicago, Illinois, 2012